*Macromolecules* **1999,** *32,* 2731−2738

# Structure of a Diblock Copolymer Adsorbed at the Hydrophobic Solid/Aqueous Interface: Effects of Charge Density on a Weak Polyelectrolyte Brush

**S. W. An, P. N. Thirtle, and R. K. Thomas***

*Physical and Theoretical Chemistry Laboratory, Oxford University, South Parks Road, Oxford OX1 3QZ, U.K.*

**F. L. Baines, N. C. Billingham, and S. P. Armes**

*School of Chemistry, Physics, and Environmental Science, University of Sussex, Falmer, Brighton BN1 9QJ, U.K.*

**J. Penfold**

*ISIS, CCLRC, Chilton, Didcot, Oxfordshire OX11 0QX, U.K.*

*Received July 21, 1998; Revised Manuscript Received December 9, 1998*

ABSTRACT: We have used neutron reflection to study the effects of pH and added electrolyte on the structure of a weak polyelectrolyte brush anchored by means of a hydrophobic block to a hydrophobic surface. The copolymer was poly(2-(dimethylamino)ethyl methacrylate-*block*-methyl methacrylate) (poly(DMAEMA-*b*-MMA)) containing 70% DMAEMA and having a molecular weight of 10000. The MMA block and the hydrophobic octadecyltrichlorosilane (OTS) layer were deuterated in order to highlight the DMAEMA fraction of the layer. The MMA block was found to bind strongly and irreversibly to a self-assembled monolayer of octadecyl trichlorosilane (OTS) on silica. The copolymer distribution could be described in terms of two uniform layers, a thin layer next to the surface containing all the MMA block and variable amounts of the DMAEMA residues with a copolymer volume fraction of about 0.8 and a more diffuse block corresponding to the polyelectrolyte brush. The presence of DMAEMA residues in the thin layer and the variation of this amount with pH and added electrolyte show that, near the anchor layer of the MMA block, the DMAEMA block is not ionized, in agreement with the model of a grafted weak polyelectrolyte proposed by Israels et al.

## Introduction

There has been much recent interest in the self-assembly of amphiphilic copolymers both in bulk solution and at interfaces. This stems partly from the wide range of surface and bulk behavior that can be generated, which makes these systems theoretically interesting and opens up a range of practical applications, and partly from the emergence of new experimental techniques capable of probing the structure of aggregates in bulk or at interfaces. The amphiphilic nature of diblock copolymers is typically manifested in self-assembly in the presence of a solvent that is selective for one of the blocks, which may give rise to the formation of aggregates such as micelles and microemulsions. It may also be manifested in the presence of a surface that is selective for one of the blocks, and this feature makes diblock copolymers valuable in colloidal stabilization and for the manipulation of surface properties. The class of polymers where one block is a polyelectrolyte and the other block is hydrophobic are particularly interesting because they are amphiphilic with respect to water and oil and, in many respects, can be considered to be macromolecular analogues of small molecule ionic surfactants, which is where the widest range of technological applications occur.

Polyelectrolytes at solid/liquid interfaces have been extensively studied during the past few years (see refs 1 and 2 for a summary). There are two main limiting cases. One is where the polyelectrolyte chain is terminally grafted to the surface forming a so-called brush. In such a system the amount of polymer attached to the surface is fixed and the polymer then has to adjust to external conditions subject to the initial packing constraint. When the electrostatic interactions become stronger, e.g., by adjusting the pH or ionic strength, the chains are forced to stretch because they cannot desorb. Another limiting situation is where there is an equilibrium between the adsorbed layer and the bulk polyelectrolyte solution. In this situation the number of polyelectrolyte chains at the interface is not fixed so that if the electrostatic repulsion is changed, the polyelectrolyte can now respond by reducing or increasing its surface density by desorption or adsorption. An intermediate situation can be created by making the polyelectrolyte one block in a diblock copolymer where the other block is neutral and has an affinity for the surface. The affinity of the neutral block for the surface may be adjusted by chemical manipulation of the surface and/or by the choice of neutral block. A strong affinity for the surface can be generated by choosing a hydrophobic neutral block and creating a hydrophobic surface. Since water is generally a good solvent for the polyelectrolyte block, this should create a situation close to the first limit outlined above. In the present paper we are concerned with just such a system but with the added possibility of controlling the charge density on the polyelectrolyte block by making it a weak polyelectrolyte and varying the pH.

In three recent papers we have described neutron reflectivity measurements on layers of the water-soluble

10.1021/ma981146+ CCC: $18.00

diblock copolymer poly(2-(dimethylamino)ethyl methacrylate-*block*-methyl methacrylate) copolymer (poly(DMAEMA-*b*-MMA); 70 mol % DMAEMA, $M_n = 10000$) adsorbed at the air/water interface.[3-5] The MMA block is water-insoluble, and the DMAEMA block is a weak polyelectrolyte whose charge density can be controlled by pH variation. At low concentrations the adsorbed layer consists of an approximately uniform distribution of the two blocks of the copolymer along the direction normal to the interface with about half of the layer immersed in the underlying water. At higher concentrations the adsorbed layer has a cross-sectional structure resembling that expected for an adsorbed micelle with the majority of the more hydrophobic MMA forming the core. In this layered structure the outer layer consists largely of the polyelectrolyte DMAEMA component of the copolymer. Neither of these structures is expected from the simple arguments given in the previous paragraph, although related observations have been made by others,[6] and collapsed states in polyelectrolyte brushes[7] or in polyelectrolyte gels[8,9] have been predicted theoretically. The effects of pH, addition of electrolyte, molecular weight, and composition on the structure and composition of the adsorbed layer were also studied, and although some of the features of the adsorption behavior are consistent with theoretical predictions, the results generally do not conform well with the types of adsorbed layers usually assumed in theoretical treatments.

The air/liquid interface bears some resemblance to the hydrophobic solid/liquid interface. For the small number of small molecule surfactant systems investigated by neutron reflection, this resemblance is confirmed by similar patterns of adsorption and similar structural characteristics of the adsorbed layer. However, the range of layer structures possible for small molecule surfactants is quite limited, and the air/liquid surface generally appears to be somewhat more disordered, particularly by thermal roughness. The combination of enhanced interaction between the surface and the hydrophobic block of the copolymer, the loss of thermal roughness, and the greater range of possible structures might disturb the balance of interactions in the diblock copolymer layer sufficiently to generate a different layer structure at the solid/liquid interface, possibly one more in accord with theoretical predictions, especially if the solid surface is made extremely hydrophobic. There is also the possibility of controlling the surface layer more precisely than at the air/water interface, where changes in the bulk solution conditions are inevitably associated with changes in concentration at the surface, which are often difficult to disentangle from structural changes. We have therefore extended the study of the structure of poly(DMAEMA-*b*-MMA) blocks to the hydrophobic solid/liquid interface.

## Experimental Details

The substrate was a single crystal of silicon with dimensions 12.7 × 5.08 × 2.54 $cm^3$, purchased from Semiconductor Processing Inc. The surface of the block was prepared using the sequence (i) lapping with 3 $\mu$m diamond polish to create a flat surface, and polishing with (ii) 1 $\mu$m diamond and (iii) 0.1 $\mu$m aluminum oxide, using a Engis polisher. After being washed with water, the silicon blocks were then put through a cleaning cycle consisting of (i) initial soaking for 20 min in neutral Decon followed by rinsing in water, (ii) immersion in 7:1 $H_2SO_4$:$H_2O_2$ for 5 min at >100 °C, followed by rinsing in water (UHQ), and (iii) treatment with ozone/UV for 1 h.[10] The self-assembled monolayer was then prepared in the following steps. The block was immersed in a freshly prepared solution of octadecyl trichlorosilane, $C_{18}D_{37}SiCl_3$ (d-OTS) in a 1:4 mixture of $CH_2Cl_2$ and *n*-hexadecane at a concentration of approximately $10^{-3}$ M for 1 h at a temperature of less than about 11 °C.[10] The block was then removed and rinsed in $CH_2Cl_2$, ethanol and water before assembling the cell for the experiment. The preparation of d-OTS and poly(DMAEMA-*b*-dMMA) blocks have been described in full elsewhere.[10,11]

The PTFE trough was cleaned by soaking it in alkaline detergent overnight and then rinsing several times with ultrapure water (Elgastat UHQ, Elga, U.K.). The pH of the solution was adjusted using hydrochloric acid and maintained constant during the measurements by keeping the samples under a nitrogen or argon atmosphere. The neutron reflection measurements were carried out on the reflectometer SURF at Rutherford Appleton Laboratory (Didcot, U.K.). The instrument and the procedure for making the measurements have been fully described elsewhere.[13]

## Results

**Neutron Reflection and Layer Composition.** In a neutron reflection experiment, the specular reflection, *R*, is measured as a function of the wave vector transfer, $\kappa$, perpendicular to the reflecting surface, where

$$\kappa = \frac{4\pi}{\lambda} \sin \theta \tag{1}$$

$\theta$ is the glancing angle of incidence and $\lambda$ the wavelength of the incident neutron beam. $R(\kappa)$ is related approximately to the scattering length density across an interface, $\rho(z)$, by

$$R(\kappa) = \frac{16\pi^2}{\kappa^2} |\hat{\rho}(\kappa)|^2 \tag{2}$$

where $\hat{\rho}(\kappa)$ is the one-dimensional Fourier transform of $\rho(z)$

$$\hat{\rho}(\kappa) = \int_{-\infty}^{+\infty} \exp(-i\kappa z)\, \rho(z)\, dz \tag{3}$$

These approximate relations show that there is a direct relation between reflectivity and structure, but it is often more convenient to use the optical matrix method[14] to calculate the reflectivity exactly for any given model of the interface. This is the method we use in the present paper. In a typical analysis, the measured data are compared with a calculated reflectivity profile with different model density profiles. A model will consist of a series of layers, each with a scattering length density $\rho$ and thickness *t*. By variation of $\rho$ and *t* for each layer, the calculated profile may be compared with the measured profile until the optimum fit to the data is found. Although any one profile may not provide a unique solution, the use of different isotopic contrasts can usually ensure that an unambiguous model of the interface is obtained.

Because hydrogen and deuterium nuclei scatter neutrons with different amplitudes, it is possible to use a combination of protonated and deuterated materials to change the reflectivity profile of a system while keeping the same chemical structure at the interface. In particular, adjustment of the H/D ratio may be used to prepare solvents which are contrast matched to the bulk silicon. The contrast between the silicon and the solvent is then zero, giving a reflectivity profile arising only from the interfacial region. The scattering length density (SLD), $\rho_a$, of a species *a* is given by the sum of the scattering lengths, $b_i$, of each component nucleus, *i*, multiplied by its number density, $\nu_i$

$$\rho_a = \sum_i \nu_i b_i \tag{4}$$

In an experiment where adsorbates $i$ are adsorbed on to a surface from aqueous solution the experimental value of the scattering length density of the adsorbed layer, $\rho_{\text{exp}}$, obtained from the model used to fit the reflectivity profile, is made up of the contributions from the materials themselves and that from water in the layer

$$\rho_{\text{exp}} = \sum \phi_i b_i \tag{5}$$

where $\phi_i$ is the volume fraction of component $i$ in the layer and $\rho_i$ the scattering length density of the pure material. The basic parameters such as scattering lengths, molecular volumes, and scattering length densities of the particular copolymer and hydrophobing agent used in this study are given in Table 1.

**Characterization of the Surface of the Substrate.** Although the oxide layer present at the silicon-(111) surface does not contribute much to the reflected signal because its scattering length density is not very different from the underlying silicon, the characterization of the hydrophobic and copolymer layers will not be reliable unless the thickness and mean composition of the oxide layer have previously been determined. We have found that the polishing and cleaning routines are sufficiently reproducible that an independently characterized surface of a separately polished and cleaned Si (111) block is of adequate accuracy. It is then sufficient to check the reflectivity profiles of any given block in $D_2O$ and water of the same scattering length density as silicon, i.e., $2.07 \times 10^{-6}$ Å $^{-2}$, which we designate as water$_{2.07}$, rather than do a full characterization. Similar considerations apply to the self-assembled monolayer of d-OTS except that there may be small variations from sample to sample. (Large variations occasionally occur, but such blocks would be discarded.) The reflectivities were indeed found to be closely similar to those from more thoroughly characterized samples,[11] and we therefore do not show the fits here. As in some earlier studies, we found that it was necessary to divide the d-OTS layer into two parts. The overall thickness of the self-assembled monolayer was found to be 26 ± 2 Å, which is the same within experimental error as the fully extended length, and the coverage of the silica was found to be 85−90%, comparable with the best values we have been able to obtain on these very large blocks. We have commented elsewhere on this value.[11] Apart from the presence of 10−15% water in the layer (from which the coverage is deduced) the presence of a significant concentration of defects in the layer is supported by the later observation that there is a small amount of penetration of the polymer into the layer (see below). The overall parameters for the adsorbing substrate are summarized in Table 2.

**Table 1. Volumes, Scattering Lengths (*b*) and Scattering Length Densities (*ρ*) for the Materials Used**

| material | vol/Å$^3$ | $b \times 10^4$/Å | $\rho \times 10^6$/Å $^{-2}$ |
|---|---|---|---|
| $H_2O$ | 30 | −0.168 | −0.56 |
| $D_2O$ | 30 | 1.915 | 6.35 |
| water$_{2.07}$ | 30 | 0.621 | 2.07 |
| $C_{18}D_{37}$ | 540 | 36.65 | 6.76 |
| Si | 20 | 0.415 | 2.07 |
| $SiO_2$ | 47 | 1.585 | 3.41 |
| MMA-$d_9$ | 140 | 9.824 | 7.02 |
| DMAEMA | 225 | 1.798 | 0.80 |

**Table 2. Parameters Used to Fit the Oxide and d-OTS Layers[a]**

| layer | thickness/ Å | $10^6\rho$/Å$^{-2}$ (in $D_2O$) | $10^6\rho_{2.07}$/Å$^{-2}$ (in water$_{2.07}$) | $\phi_{SiO_2}$ | $\phi_{dOTS}$ |
|---|---|---|---|---|---|
| oxide | 20 | 4.0 | 3.5 | 0.81 | 0.07 |
| d-OTS(1) | 14 | 6.1 | 5.1 | | 0.79 |
| d-OTS(2) | 12 | 5.3 | 4.1 | | 0.72 |

[a] $\rho$ is scattering length density, $\phi$ is volume fraction, and any residual volume is occupied by water.

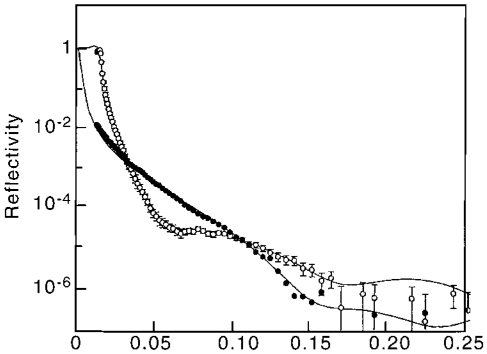

**Figure 1.** Neutron reflectivity profiles for poly(DMAEMA-*b*-dMMA) adsorbed on the hydrophobic Si/$SiO_2$/d-OTS surface in $D_2O$ (○) and water$_{2.07}$ (●) at pH 7.5. The continuous lines are the best fits of profiles calculated using the parameters given in Table 3.

**Structure of the Adsorbed Copolymer Layer.** The extent of adsorption of the copolymer onto the hydrophobic d-OTS surface was assessed by measuring reflectivity profiles in the presence of $D_2O$ after exposure of the surface to copolymer solution and after rinsing with dilute HCl and water. As we have discussed elsewhere, the choice of a deuterated hydrophobic layer creates a particularly favorable scattering length density profile when largely protonated materials are adsorbed. The contrast between the adsorbed protonated layer and the two layers on either side of it is then high when $D_2O$ is the solvent, and the reflectivity becomes very sensitive to any adsorbed material. The reflectivity profiles measured from adsorbed copolymer in $D_2O$ and in water$_{2.07}$ both at pH 7.5 are shown in Figure 1 together with the best fitted curves for a five-layer model. The reflectivity is strongly modified by the presence of the copolymer layer. The first three layers in the model represent the oxide layer and the two sublayers of the OTS layer, and apart from a small adjustment because of some penetration of the OTS layer by the copolymer, their parameters were fixed by the analysis described in the previous section. The only unknowns in the five-layer model are therefore those for the two layers representing the copolymer distribution. The polymer was found to consist of two layers: first, a thin, compact layer containing all the MMA segments and some of the DMAEMA segments, and second, a diffuse layer, which contains only DMAEMA and water. The former is essentially an anchoring layer, and the latter has some of the characteristics of a polymer brush. From now on we refer to them as the anchor and brush layers, respectively. The anchor layer is only some 7 ± 1 Å thick and the brush about 30 Å thick. The reflectivity profiles at the end of the experiment, after several changes of pH and after rinsing were found to be identical with those shown in Figure 1, demonstrating that the copolymer layer retained its

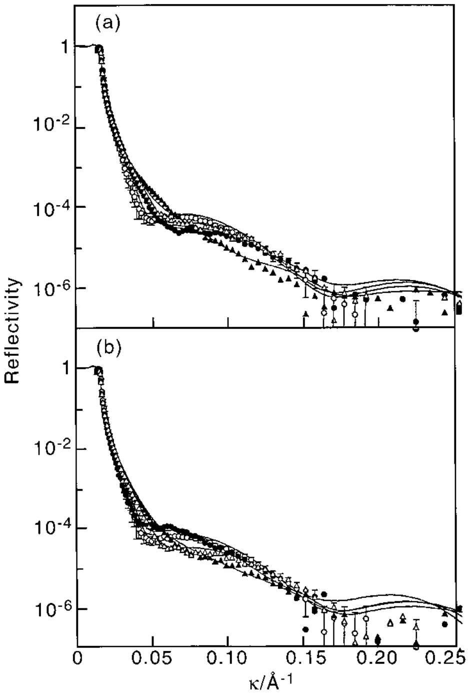

**Figure 2.** Neutron reflectivity profiles for poly(DMAEMA-*b*-dMMA) adsorbed on the hydrophobic Si/SiO$_2$/d-OTS surface in D$_2$O at various pH: (a) pH 11 (△), pH 9.5 (○), pH 7.5 (●), and pH 3 (▲); (b) pH 10 (△), pH 9.5 (○), pH 8.5 (●), and pH 4 (▲). The continuous lines are profiles calculated using the parameters given in Table 3.

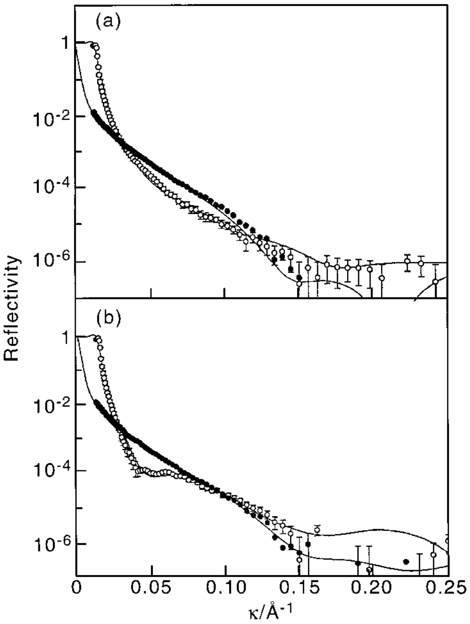

**Figure 3.** Neutron reflectivity profiles for poly(DMAEMA-*b*-dMMA) adsorbed on the hydrophobic Si/SiO$_2$/d-OTS surface in D$_2$O (○) and water$_{2.07}$ (●) at (a) pH 3 and (b) pH 8.5. The continuous lines are the best fits of profiles calculated using the parameters given in Table 3.

**Table 3. Parameters Used to Fit the Reflectivity from the Interface at Different pH**[a]

| layer | thickness/ Å | $10^6\rho$/Å$^{-2}$ (D$_2$O) | $10^6\rho$/Å$^{-2}$ (water$_{2.07}$) | $\phi_{\rm MMA}$ | $\phi_{\rm DMAEMA}$ |
|---|---|---|---|---|---|
| SiO$_2$ | 20 | 4.0 | 3.5 | | |
| d-OTS(1) | 14 | 5.9 | 4.9 | | |
| d-OTS(2) | 12 | 5.0 | 4.0 | | |
| pH 3 anchor | 4 ± 1 | 5.0 | 4.0 | 0.46 | 0.30 |
| brush | 40 ± 5 | 6.0 | 2.0 | 0.0 | 0.07 |
| pH 4 anchor | 5 | 4.8 | | 0.43 | 0.35 |
| brush | 35 | 6.0 | | 0.0 | 0.08 |
| pH 5 anchor | 6 | 3.8 | | 0.32 | 0.48 |
| brush | 32 | 6.0 | | 0.0 | 0.08 |
| pH 6 anchor | 6 | 4.0 | | 0.27 | 0.46 |
| brush | 30 | 6.0 | | 0.0 | 0.08 |
| pH 7.5 anchor | 7 | 4.0 | 2.8 | 0.27 | 0.45 |
| brush | 30 | 6.0 | 2.0 | 0.0 | 0.08 |
| pH 8.5 anchor | 8 | 3.8 | 2.9 | 0.27 | 0.49 |
| brush | 27 | 5.7 | 1.9 | 0.0 | 0.12 |
| pH 9.5 anchor | 9 | 3.5 | 2.7 | 0.26 | 0.53 |
| brush | 21 | 5.5 | 1.9 | 0.0 | 0.15 |
| pH 10 anchor | 7 | 3.3 | | 0.25 | 0.58 |
| brush | 22 | 5.9 | | 0.0 | 0.09 |
| pH 11 anchor | 8 | 3.2 | | 0.24 | 0.60 |
| brush | 20 | 5.8 | | 0.0 | 0.10 |

[a] $\rho$ is scattering length density, $\phi$ is volume fraction, and any residual volume is occupied by water.

integrity throughout the experiments. Thus the polymer is strongly and irreversibly adsorbed and the adsorbed amount was found to be 1.3 ± 0.3 mg m$^{-2}$.

Figure 2 shows the effect of varying the pH on the reflectivity in D$_2$O. As already noted, this contrast is very sensitive to the nature of the polymer layer, and it can be seen that the reflectivity varies substantially with pH, although the amount of adsorbed polymer is constant. The implication must be that the structure of the layer also changes significantly with pH. The reflectivity at pH 7.5 was fitted with a two-layer model for the copolymer (Figure 1), and in principle, this is sufficient for the determination of the layer structure. However, the use of a second, independent profile at different isotopic composition greatly reduces any ambiguities in the derived structure. The reflectivities at some of the pH values were therefore also recorded in water$_{2.07}$. Two pairs of reflectivity profiles at the two different contrasts with the best fits of a two-layer model to the data are shown in Figure 3. The fitted parameters are given for all pH in Table 3 with the derived compositions.

Several trends may be identified from the fitted data. The thickness of the anchor layer increases with pH up to about pH 9, and then it starts to decrease again (Figure 4). The DMAEMA block is a weak electrolyte (p$K_a \approx 7.3$), and its charge density varies with pH. The reason for the increase in thickness of the anchor layer is that the fraction of DMAEMA residues in the anchor layer increases as it becomes less charged with increasing pH up to pH 9 and then a slight compaction of the film occurs above pH 9. These changes can be so precisely identified for three reasons. First, the interference effect observed in the reflectivities of Figure 2 is mainly generated by the anchor layer creating a contrast for the whole d-OTS layer, and then the interference is from the combined thickness of these two layers. Second, since the MMA block is deuterated and its scattering length density is similar to that of the d-OTS, the presence of hDMAEMA in the anchor layer has a large effect on the overall contrast of the d-OTS layer. Third, any compaction of the copolymer in the layer changes the volume fraction of water, and the combined measurements in D$_2$O and water$_{2.07}$ are sensitive to the volume fraction of water. As shown in Figure 4 the thickness of the brush layer generally increases as the pH decreases. However, there is a greater uncertainty in the determination of the thickness of this layer because the effects of the brush on the reflectivity, which are generally most significant in the lower range of $\kappa$, as is seen by comparison of the D$_2$O profiles at pH 9.5

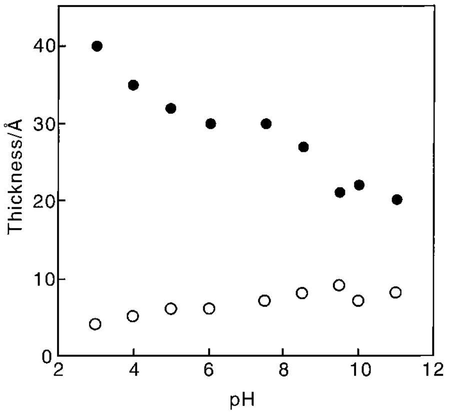

**Figure 4.** Variation of thickness of brush (●) and anchor (○) layers with pH for poly (DMAEMA-*b*-dMMA) adsorbed on the hydrophobic Si/SiO$_2$/d-OTS surface.

and 11, are always much less than the effects of the anchor layer. Nevertheless, the results are generally consistent with the stoichiometry of the copolymer, without the need to apply the stoichiometry as a constraint in the fitting procedure, as was found to be necessary for the equivalent layers at the air/water interface.[3,4] We have divided the copolymer layer into just two layers because that is the minimum required to fit the whole set of data. However, the division between the two layers may not be as sharp as this procedure implies.

The observed changes in the structure of the layer are qualitatively as would be expected from the pattern of ionization on the DMAEMA block. We have already shown that the p$K_a$ of the DMAEMA block is 7.3, and therefore it will be half-charged at this pH.[15] Charged DMAEMA segments are hydrophilic, and uncharged ones are hydrophobic. At lower pH, DMAEMA segments therefore desorb from the anchor layer into the brush region because they are more hydrophilic. This, combined with the increased electrostatic repulsion between the more strongly ionized segments in the brush layer, causes an increase in the thickness of the brush layer. This is a different situation from that usually considered in theoretical treatments where the brush and anchor blocks are normally assumed not to mix. At high pH there will be a tendency for the whole layer to collapse because the DMAEMA segments will lose their charge and become hydrophobic. However, there is clearly a limit to the collapse, which must result from the high entropic penalty of total collapse. The layer appears to reach a limiting thickness with a small fraction of the DMAEMA block generating a diffuse tail. At these densities the brush layer can no longer be regarded as a typical brush, but more like a “mushroom”.

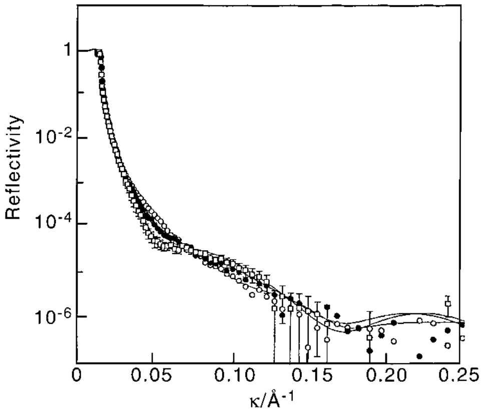

**Figure 5.** Neutron reflectivity profiles for poly (DMAEMA-*b*-dMMA) adsorbed on the hydrophobic Si/SiO$_2$/d-OTS surface in D$_2$O at pH 3 and different ionic strengths, no added electrolyte (○), 1 M NaCl (●), and 5 M NaCl (□). The continuous lines are calculated using the parameters in Table 4.

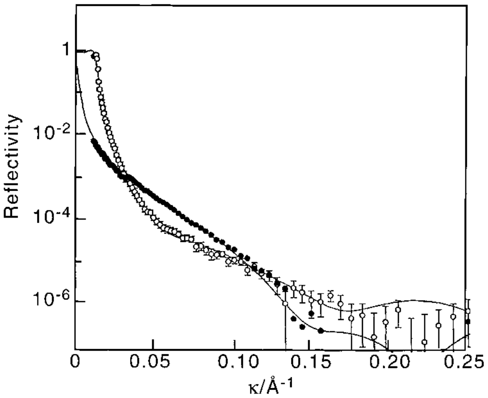

**Figure 6.** Neutron reflectivity profiles for poly (DMAEMA-*b*-dMMA) adsorbed on the hydrophobic Si/SiO$_2$/d-OTS surface in D$_2$O (○) and water$_{2.07}$ (●) at pH 3 in the presence of 1 M NaCl. The continuous lines are the best fits of profiles calculated using the parameters given in Table 4.

**Table 4. Parameters Used To Fit the Reflectivity from the Interface at pH 3 and Different Ionic Strengths**[a]

| layer | thickness/ Å | $10^6\rho$/ Å$^{-2}$ (D$_2$O) | $10^6\rho$/ Å$^{-2}$ (water$_{2.07}$) | $\phi_{\mathrm{MMA}}$ | $\phi_{\mathrm{DMAEMA}}$ |
|---|---|---|---|---|---|
| SiO$_2$ | 20 | 4.0 | 3.5 | | |
| d-OTS(1) | 14 | 5.9 | 5.0 | | |
| d-OTS(2) | 12 | 5.0 | 4.0 | | |
| salt free anchor | 4 ± 1 | 5.0 | 4.0 | 0.46 | 0.30 |
| brush | 40 ± 5 | 6.0 | 2.0 | 0.0 | 0.07 |
| 0.1 M NaCl anchor | 4 | 5.0 | 4.0 | 0.46 | 0.30 |
| brush | 38 | 6.0 | 2.0 | 0.0 | 0.07 |
| 1 M NaCl anchor | 6 | 4.5 | | 0.39 | 0.38 |
| brush | 30 | 6.0 | | 0.0 | 0.07 |
| 3 M NaCl anchor | 6 | 4.0 | | 0.28 | 0.45 |
| brush | 24 | 5.8 | | 0.0 | 0.10 |
| 5 M NaCl anchor | 6 | 4.0 | | 0.28 | 0.45 |
| brush | 24 | 5.8 | | 0.0 | 0.11 |

[a] $\rho$ is scattering length density, $\phi$ is volume fraction, and any residual volume is occupied by water.

Figure 5 shows the neutron reflectivity profiles from the copolymer layer in D$_2$O at pH 3 and at several salt concentrations (0.1, 1, 3, and 5 M NaCl). The effect of adding salt is qualitatively similar to that of increasing the pH; i.e., the overall thickness of the layer decreases in thickness, and the amount of copolymer in the anchor layer increases. These changes were determined accurately, using fits of the two-layer copolymer structure to the reflectivity data from D$_2$O and from water$_{2.07}$. An example of one pair of fits is shown in Figure 6, and the fitting parameters and derived compositions are given in Table 4. These confirm the qualitative conclusion above. The thickness of the anchoring layer and the volume fraction of DMAEMA residues in this layer both increase as the addition of salt increases the electrostatic screening and makes the DMAEMA block behave more hydrophobically. The brush decreases in thickness, reaching a limiting thickness comparable to the value reached at high pH.

Figure 7 shows the effects of salt on the reflectivity from the adsorbed copolymer layer at pH 9.5 in D$_2$O, and Figure 8 shows the best fits of the two-layer model

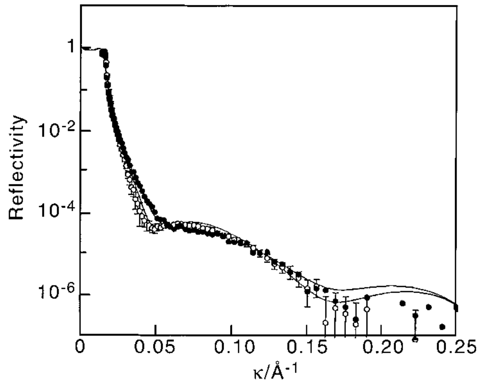

**Figure 7.** Neutron reflectivity profiles for poly (DMAEMA-*b*-dMMA) adsorbed on the hydrophobic Si/SiO$_2$/d-OTS surface in D$_2$O at pH 9.5 in the absence (○) and presence (●) of 1 M NaCl. The continuous lines are calculated using the parameters of Table 5.

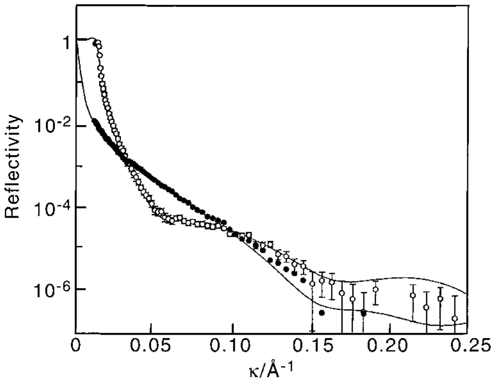

**Figure 8.** Neutron reflectivity profiles for poly (DMAEMA-*b*-dMMA) adsorbed on the hydrophobic Si/SiO$_2$/d-OTS surface in D$_2$O (○) and water$_{2.07}$ (●) at pH 9.5 in the presence of 1 M NaCl. The continuous lines are the best fits of profiles calculated using the parameters given in Table 5.

**Table 5. Parameters Used to Fit the Reflectivity from the Interface at pH 9.5 and Different Ionic Strengths**[a]

| layer | thickness/ Å | $10^6\rho$/ Å$^{-2}$ (D$_2$O) | $10^6\rho$/Å$^{-2}$ (water$_{2.07}$) | $\phi_{MMA}$ | $\phi_{DMAEMA}$ |
|---|---|---|---|---|---|
| SiO$_2$ | 20 | 4.0 | 3.5 | | |
| d-OTS(1) | 14 | 6.0 | 5.0 | | |
| d-OTS(2) | 12 | 5.0 | 4.0 | | |
| salt free anchor | 9 | 3.5 | 2.7 | 0.26 | 0.53 |
| brush | 21 | 5.5 | 1.9 | 0.0 | 0.15 |
| 0.1 M NaCl anchor | 8 | 3.6 | 2.5 | 0.24 | 0.52 |
| brush | 25 | 5.8 | 2.0 | 0.0 | 0.10 |
| 1 M NaCl anchor | 8 | 3.7 | 2.7 | 0.28 | 0.51 |
| brush | 25 | 5.9 | 2.0 | 0.0 | 0.09 |

[a] $\rho$ is scattering length density, $\phi$ is volume fraction, and any residual volume is occupied by water.

to the pair of reflectivity profiles at 1 M NaCl in D$_2$O and in water$_{2.07}$, for which the fitted parameters and derived compositions are given in Table 5. The effect of added electrolyte is now quite different from that at pH 3. The effects of addition of salt are small, and if anything, the extra salt causes the anchor layer to become thinner and the DMAEMA chains to become slightly more extended in the brush layer. At first sight, these effects are the opposite of what would be expected from the normal screening effect of electrolyte. However, in the absence of salt the brush is almost neutral, and the only possibilities are that addition of electrolyte may affect the solvent quality and that it will enhance the ionization of a weak polyelectrolyte. At this pH, the charge density on the DMAEMA block is sufficiently low that screening is unimportant but may still be sufficient that the electrolyte can enhance the ionization; i.e., addition of electrolyte would be equivalent to a slight lowering of the pH. It is easy to estimate this effect. At 1 M NaCl the mean activity coefficient is about 0.66.[16] For the dissociation of a monomeric acid, the maximum effective increase in ionization to accommodate this decrease would be approximately 1/0.66, i.e., a 50% increase. At low levels of dissociation this corresponds to a pH about 0.2 units lower. The effect is consistent with a small shift of about this magnitude.

## Discussion

Although the length of the DMAEMA polyelectrolyte brush is not long enough for it to be appropriate to apply quantitative theoretical models to interpret its structure, there are some features of the adsorption which are qualitatively consistent with some of the predictions that have been made. We start by summarizing the predictions for a polyelectrolyte brush. Pincus[17] used scaling arguments to show that a fairly dense array of polyelectrolyte chains grafted to a surface could be in two limiting states. In the first, the electrolyte concentration is such that the Debye length is shorter than the thickness of the brush and the counterions are then located within the brush and cause it to swell by their gain in entropy on swelling (osmotic swelling). In the second state, the Debye length is longer than the thickness of the brush and the counterions are expelled from the brush. The counterions essentially then see the polyelectrolyte brush as part of a charged surface. In this “bare brush” regime, which only exists for low fractional charge densities, the thickness is much more sensitive to the number of polymer segments. On addition of electrolyte to the brush when it is in the osmotic swelling regime, the added electrolyte screens the charges and the thickness of the brush reverts to a form similar to that for a neutral brush but with an effective virial coefficient determined by the electrostatic interactions, the salted brush. Pincus did not include excluded volume interactions in his treatment, and later Borisov et al.[18] showed that these may dominate the electrostatic interactions at high grafting densities. Ross and Pincus[7] and Zhulina et al.[19] have shown that the solvent quality is only important when it drops below the Θ condition, when the brush may collapse completely. Israels et al.[20] studied charged polymeric brushes using a self-consistent mean field model, and while their analysis supports most of the above conclusions, they found that the bare brush regime was unlikely to occur with any reasonable set of parameters. They also extended the theory to weak grafted polyelectrolytes and found that the high potential present within the brush is too large for the weak electrolyte to dissociate properly.[21] The degree of ionization is then predicted to decrease on moving toward the point where the polyelectrolyte is attached to the surface, with the brush progressively behaving more like a neutral polymer. The addition of salt may then assist ionization by reducing the potential before causing the system to move into the more collapsed state characteristic of the salted brush. The brush length of a weak polyelectrolyte may therefore pass through a maximum on addition of electrolyte. Lyatskaya et al.[22] have since developed an analytical self-consistent field theory for a weak polyacid as a function of pH and electrolyte concentration which is

**Table 6. Parameters of the Copolymer Layer under Different Conditions**

| conditions | no. of segments in brush | nominal fractional charge[a] | thickness/ Å |
|---|---|---|---|
| pH 3 | 34 | 1.0 | 40 |
| pH 4 | 29 | 1.0 | 35 |
| pH 5 | 23 | 1.0 | 32 |
| pH 6 | 22 | 0.85 | 30 |
| pH 7.5 | 21 | 0.45 | 30 |
| pH 8.5 | 22 | 0.10 | 27 |
| pH 9.5 | 19 | 0 | 21 |
| pH 10 | 16 | 0 | 22 |
| pH 11 | 14 | 0 | 20 |
| pH 3/1 M NaCl | 23 | 1.0 | 30 |
| pH 3/5 M NaCl | 24 | 1.0 | 24 |
| pH 9.5/1 M NaCl | 17 | 0 | 25 |

[a] Based on the bulk ionization as measured directly.

in good agreement with the numerical results of Israels et al.

At the air/water interface it was found that there was extensive overlap between the distributions of the MMA and DMAEMA blocks at low coverage. As pointed out by An et al. it is not possible to distinguish true mixing of the two components from lateral segregation in the same plane because neutron reflection is not sensitive to the in-plane structure. The same is true at the solid/liquid interface but now the difference is that there is a well-defined anchor film which is both thin and contains all the MMA. The additional and variable amount of DMAEMA chains that are incorporated into this anchor layer under different conditions may mix with the MMA blocks, or they may form separate microdomains on the surface. The interleaving MMA and DMAEMA domains would not be distinguishable by neutron reflection. The number of DMAEMA chains incorporated into the anchor layer is always such as to keep the total polymer volume fraction in the layer approximately constant at about 0.8. Since the thickness of this layer varies, the number of DMAEMA segments in the polyelectrolyte brush part of the layer also varies, even though the grafting density is always constant at about 1280 Å$^2$ per chain. Table 6 compares the number of segments in the brush layer with the observed thickness of this layer and the charge fraction on the polyelectrolyte calculated on the basis that each DMAEMA group ionizes independently and that the mean p$K_a$ is 6.7 (the value found for the air/liquid interface).

As the pH increases from 3 to 5, a range over which the polyelectrolyte is nominally completely dissociated, the polyelectrolyte brush not only collapses (from 40 to 32 Å; see Table 6) but a significant, and increasing, fraction is incorporated into the anchor region. Both of these effects must be associated with a decrease in the ionization of the copolymer. The incorporation of DMAEMA chains into the anchor layer indicates that the ionization of the DMAEMA residues is reduced to a very low value in the immediate vicinity of the surface. This is consistent with the effect predicted for a weak polyelectrolyte by Israels et al.,[21] where the degree of ionization progressively decreases closer to the surface. The low degree of ionization may also be enhanced by the lower dielectric constant in the anchor layer resulting from the high volume fraction of polymer.[8] As commented on above, the division into high volume fraction anchor layer and brush is somewhat artificial and reflects the low resolution of the experiment. The actual distribution is probably more gradual. From pH 5 to 8.5, where the ionization of the DMAEMA is nominally changing quite rapidly, the state of both anchor and brush layers remains, surprisingly, approximately constant. This cannot be because the neutral brush limit has been reached, where the DMAEMA segments would be interacting purely through excluded volume effects. If this were the case, the further collapse of the layer when the pH rises above 9 would not occur. In the region pH 5−8.5, the charge density on the polyelectrolyte should be low and the effect of the high potential, which is what limits the overall charge in the layer, may not be as great. Thus, a low and relatively constant charge may be maintained over a range of pH where the nominal change is quite large. This could therefore be an example of the charge regulation discussed by Israels et al. Above pH 9, the DMAEMA block is nominally almost not ionized and a maximum amount is incorporated into the anchor layer. This reduces the number of segments in the brush layer, whose thickness is presumably maintained by excluded volume interactions (neutral brush regime).

The effect of added salt at pH 3, where the charge density on the DMAEMA block should be a maximum, is to cause a partial collapse of the layer. The characteristics of the layer structure at the highest salt concentration are different from that of the uncharged layer and are consistent with a rather higher excluded volume interaction. This is consistent with the general expectation that the interactions in the salted polyelectrolyte brush should be somewhat larger than the simple excluded volume interactions. Added electrolyte at pH 9.5 has a relatively small effect on the adsorbed copolymer layer, if anything causing it to swell slightly. There may be some residual ionization at this pH, which would be increased by the presence of electrolyte, as discussed in the previous section. However, the effect is almost within the experimental error.

The molecular weight of the copolymer is too small to provide a quantitative test of the predictions of Israels et al. However, the various effects of pH and added electrolyte are qualitatively consistent with the predictions of Israels et al., in particular that there must be a gradient in the extent of ionization in the layer, and the latter, as far as the authors are aware, has not previously been established experimentally. It would also have been interesting to test whether the predictions of Israels et al.[21] hold for the air/water interface, but the more complex structure observed at the latter interface prevents such a comparison.

**Acknowledgment.** F.L.B. wishes to thank the School of Chemistry, Physics, and Environmental Science, University of Sussex, and Courtaulds Research for financial support in the form of a D.Phil. studentship. S.P.A. and N.C.B. acknowledge the EPRSC for continued support of their water-soluble polymers research program at Sussex. R.K.T. also thanks the EPSRC for support.

## References and Notes

(1) Fleer, G. J.; Cohen Stuart, M. A.; Scheutjens, J. M. H. M.; Cosgrove, T.; Vincent, B. *Polymers at Interfaces*; Chapman & Hall: London, 1993.

(2) Fleer, G. J. *Ber. Bunsen-Ges. Phys. Chem.* **1996**, *100*, 936−942.

(3) An, S. W.; Su, T. J.; Thomas, R. K.; Baines, F. L.; Armes, S. P.; Billingham, N. C.; Penfold, J. *J. Phys. Chem. B* **1998**, *102*, 387−393.

(4) An, S. W.; Thomas, R. K.; Baines, F. L.; Armes, S. P.; Billingham, N. C.; Penfold, J. *J. Phys. Chem. B* **1998**, *102*, 5120−5126.

(5) An, S. W.; Thomas, R. K.; Baines, F. L.; Armes, S. P.; Billingham, N. C.; Penfold, J. *Macromolecules* **1998**, *31*, 7877−7885.

(6) Li, Z.; Zhao, W.; Quinn, J.; Rafailovich, M. H.; Sokolov, J.; Lennox, R. B.; Eisenberg, A.; Wu, X. Z.; Kim, M. W.; Sinha, S. K.; Tolan, M. *Langmuir* **1995**, *11*, 4785−4792.

(7) Ross, R. S.; Pincus, P. *Macromolecules* **1992**, *25*, 2177−2183.

(8) Khokhlov, A. R.; Kramarenko, E. Y. *Macromolecules* **1996**, *29*, 681−685.

(9) Khokhlov, A. R.; Kramarenko, E. Y. *Macromol Theory Simul.* **1994**, *3*, 45−59.

(10) Parikh, A. N., Allara, D. L., Azouz, I. B., Rondelez, F. *J. Phys. Chem.* **1994**, *98*, 7577−7590.

(11) Fragneto, G., Lu, J. R., McDermott, D. C., Thomas, R. K., Rennie, A. R.. Gallagher, P. D., Satija, S. K. *Langmuir* **1996**, *12*, 477−486.

(12) F. L. Baines; Armes, S. P.; Billingham, N. C.; Tuzar, Z. *Macromolecules* **1996**, *29*, 8151−8159.

(13) Penfold, J.; Richardson, R. M.; Zarbakhsh, A.; Webster, J. R. P.; Bucknall, D. G.; Rennie, A. R.; Jones, R. A. L.; Cosgrove, T.; Thomas, R. K.; Higgins, J. S.; Fletcher, P. D. I.; Dickinson, E.; Roser, S. J.; McLure, I. A.; Hillman, R. A.; Richards, R. W.; Staples, E. J.; Burgess, A. N.; Simister, E. A.; White, J. W. *J. Chem. Soc., Faraday Trans.* **1997**, *93*, 3899−3917.

(14) Heavens, O. S. Optical Properties of Thin Films; Dover: New York, 1955.

(15) An, S. W.; Thomas, R. K. *Langmuir* **1997**, *13*, 6881−6883.

(16) Robinson, R. A.; Stokes, R. H. *Electrolyte Solutions*, 2nd ed.; Butterworths: London, 1959.

(17) Pincus, P. *Macromolecules* **1991**, *24*, 2912−2919.

(18) Borisov, O. V.; Birshtein, T. M.; Zhulina, E. B. *J. Phys. II* **1991**, *1*, 521−526.

(19) Zhulina, E. B.; Borisov, O. V.; Birshtein, T. M. *J. Phys. II*, **1992**, *2*, 63−74.

(20) Israels, R.; Leermakers, F. A. M.; Fleer, G. J.; Zhulina, E. B. *Macromolecules* **1994**, *27*, 3249−3261.

(21) Israels, R.; Leermakers, F. A. M.; Fleer, G. J. *Macromolecules* **1994**, *27*, 3087−3093.

(22) Lyatskaya, Y. V.; Leermakers, F. A. M.; Fleer, G. J.; Zhulina, E. B.; Birshtein, T. M. *Macromolecules* **1995**, *28*, 3562−3569.

MA981146+